ACS APPLIED MATERIALS & INTERFACES

Research Article

www.acsami.org

Magnetic Relaxation Switch Detecting Boric Acid or Borate Ester through One-Pot Synthesized Poly(vinyl alcohol) Functionalized Nanomagnetic Iron Oxide

Guilong Zhang,[†,‡,⊥] Shiyao Lu,[†,⊥] Junchao Qian,[∥] Kai Zhong,[∥] Jianming Yao,[†] Dongqing Cai,[*,†] Zhiliang Cheng,[*,§] and Zhengyan Wu[*,†]

[†]Key Laboratory of Ion Beam Bioengineering Hefei Institutes of Physical Science, Chinese Academy of Sciences and Anhui Province, Hefei, 230031, People's Republic of China

[‡]University of Science and Technology of China, Hefei 230026, People's Republic of China

[§]Department of Bioengineering, University of Pennsylvania, 240 Skirkanich Hall, 210 South 33rd Street, Philadelphia, Pennsylvania 19104, United States

[∥]High Magnetic Field Laboratory, Hefei Institutes of Physical Science, Chinese Academy of Sciences, Hefei, 230031, People's Republic of China

ABSTRACT: We developed a highly efficient magnetic relaxation switch (MRS) system based on poly(vinyl alcohol) functionalized nanomagnetic iron oxide (PVA@NMIO) particles for the detection of boric acid or borate ester (BA/BE). It was found that the addition of BA/BE induced the aggregation of PVA@NMIO particles, resulting in a measurable change in the T_2 relaxation time in magnetic resonance measurements. The main mechanism was proposed that the electron-deficient boron atoms of BA/BE caused the aggregation of PVA@NMIO particles through covalent binding to the hydroxyl groups of PVA. This novel detection system displayed excellent selectivity, high sensitivity, and rapid detection for BA/BE. Thus, this system may provide a great application prospect for detection of BA/BE.

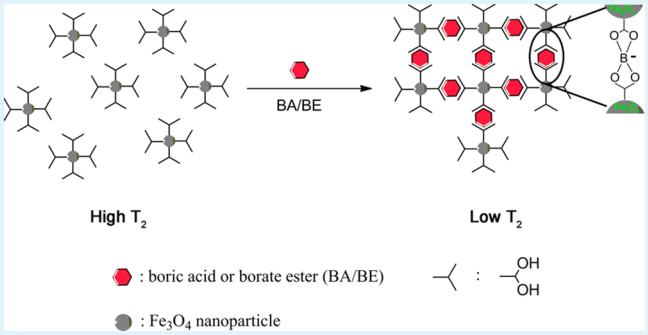

KEYWORDS: *magnetic relaxation switch, boric acid or borate ester, food additives, high selectivity, high-throughput detection*

INTRODUCTION

Boron is an essential trace element to maintain the organism health of human beings and animals, and it has also been shown to be beneficial to many other species.[1] The boron atom has a high affinity with oxygen and presents in the form of boric acid (BA), borate, or borate ester (BE) in nature.[2] Soluble forms of boron include $B(OH)_3$, $B(OH)_4^-$, and the low-level ester of borate, while the dominant form depends upon the characteristics of the solvent. The BA and BE were previously used as food additives in China because they possessed excellent antiseptic effects and could increase the taste of food.[3,4] However, once excessive BA or BE (BA/BE) was taken into a body, chemical damage to multiple organs could occur.[5] Recently, the addition of BA/BE to foods has been inhibited by the Food and Drug Administration of China; however, sometimes illegal behavior of adding BA/BE into food products still exists. Thus, it would be desired to develop some methods to detect BA/BE.

Currently, a wide range of analytical techniques have been developed to detect BA/BE.[3,6,7] Some of the most widely used methods include spectrophotometry, inductively coupled plasma spectrometry, and high performance liquid chromatography techniques.[8,9] Some methods are accurate and versatile; however, they still suffer from a few shortcomings, including complicated sample preparation, slow detection, and interference by other substances. It would be desirable to develop a new assay that is more efficient and reliable for BA/BE detection.

Contrast agents are often used to assist disease detection in magnetic resonance (MR) imaging. Among them, nanomagnetic iron oxide (NMIO) particles have been becoming an important class of MR contrast agents in the clinic, which are efficient at dephasing the spins of surrounding water protons and then enhancing spin−spin relaxation times (T_2 relaxation times).[10−12] Several recent studies showed that the aggregated NMIO presented lower T_2 relaxation times than that of the monodispersed NMIO, which acted as a magnetic relaxation switch (MRS) to detect molecular interactions.[13−15] Using NMIO as a highly efficient MRS requires a particle to be highly monodisperse in aqueous solution. To this end, the surface of a NMIO nanoparticle is usually modified with appropriate materials.[16,17] However, many methods for the

Received: June 3, 2015
Accepted: July 14, 2015
Published: July 14, 2015

DOI: 10.1021/acsami.5b04863
ACS Appl. Mater. Interfaces 2015, 7, 16837−16841

postmodification of the formed NMIO are time-consuming and costly because multiple additional steps are required.[18] Moreover, some surface modification might affect the magnetization of NMIO and reduce the sensitivity of T_2 signal changes.[19,20] Thus, it is necessary to develop a facile synthesis route for simultaneous formation and surface functionalization of NMIO.

Currently, MRSs have been mostly used to detect mRNA,[13] stereo isomers of organic substances,[14] restriction enzymes,[21] and other biomolecules.[22,23] In this work, we have developed a highly efficient T_2 contrast agent based on NMIO as a MRS to detect BA/BE. A poly(vinyl alcohol) functionalized NMIO (PVA@NMIO) displaying high transverse relaxivity and excellent monodispersity was in situ synthesized. Due to covalent binding between the hydroxyl groups of PVA and BA/BE, the addition of BA/BE induced the aggregation of PVA@NMIO in the solution, resulting in a reduction of T_2 relaxation time (Figure 1). This PVA@NMIO as a MRS showed specificity and rapid response to BA/BE.

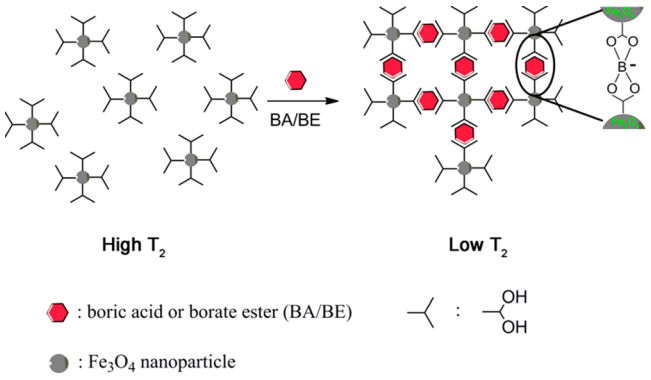

Figure 1. Schematic diagram for MRS detection of BA/BE based on PVA@NMIO.

EXPERIMENTAL SECTION

Materials. PVA, glucose, $FeCl_3$ and $FeCl_2$ were purchased from Sinopharm Co. (Shanghai, China). Boric acid, $NaBF_4$, trimethyl borate and tributyl borate (two kinds of popular BEs as the model BE) were received from Aladdin Co. (Shanghai, China). All chemical reagents were used as received without further purification.

Preparation of PVA@NMIO particles. $FeCl_3$ (0.54 g) and $FeCl_2$ (0.2 g) were dissolved in distilled water (200 mL). PVA solution (1%, 100 mL) was then added into the resulting solution followed by an agitation at 80 °C for 30 min. After that, ammonia (28% w/w, 10 mL) was added into the mixture solution with an agitation for 2 h. The obtained black product (PVA@NMIO particle) was centrifuged, and the pellet was resuspended in distilled water to make a colloidal solution of PVA@NMIO as MRS probe.

MRS assay. Different analytes including $NaBF_4$, glucose, BA, trimethyl borate and tributyl borate were added to the colloidal solution of PVA@NMIO (10 μg/mL). T_2 relaxation times of these mixed samples at different time were measured using a 9.4 T superconducting magnet by performing T_2-weighted multiecho spin echo sequence with the following parameters: repetition time (TR) of 2500 ms and 20 echoes with variable echo times (TE) ranging from 10 to 200 ms.

Characterization. The morphologies of samples were observed on an H-800 transmission electron microscope (TEM) (Hitachi Co., Japan). Particle size distribution measurements were conducted on a dynamic light scattering (DLS) detector (Malvern, UK). The structure and interaction were analyzed using a Fourier transform infrared (FTIR) spectrometer (Nicolet Co., USA). Magnetic behavior of nanoparticle was measured by superconducting quantum interference device (SQUID) magnetometer (Bruker Biospoin GmbH, Germany). T_2 relaxation time of samples was measured using a 9.4 T 8.9 cm wide bore, actively screened, vertical bore MR spectrometer (Bruker Biospoin GmbH, Germany).

RESULTS AND DISCUSSION

Nanosized PVA@NMIO was fabricated through a chemical coprecipitation method of mixing $FeCl_3$ and $FeCl_2$ in 0.3% PVA solution. The core of the obtained NMIO was around 12 nm in diameter (Figure 2a). After the core was successfully coated

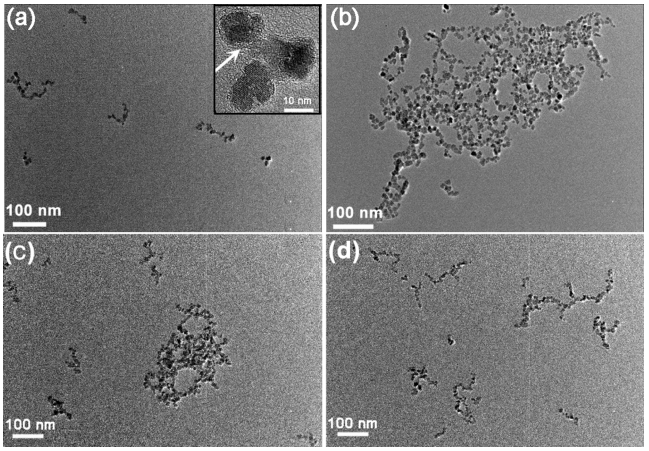

Figure 2. TEM images of PVA@NMIO (a) and PVA@NMIO after adding BA (b), trimethyl borate (c), and tributyl borate (d) in the same amounts. Inset of (a): the amplified image of PVA@NMIO.

with a layer of PVA (white arrows of the inset in Figure 2a), the whole particle increased in size to ~20 nm. The PVA@NMIO particles were stable in solution without precipitation for at least 3 months and appeared well-dispersed when observed by transmission electron microscopy (Figure 2a). However, as shown in Figure 2b, upon addition of BA to well-dispersed PVA@NMIO solution, the nanoparticles gradually self-aggregated to form clusters with larger size because of the covalent binding between hydroxyl groups of PVA@NMIO and BA/BE (illustrated by the marked oval region in Figure 1). Moreover, nanoclusters with various sizes formed after the addition of different boric compounds (Figure 2). Therein, the addition of boric acid could make the well-dispersed PVA@NMIO to be aggregated, resulting in clusters with the largest sizes. When trimethyl borate and tributyl borate were introduced to the PVA@NMIO solution, the formed nanoclusters displayed relatively small sizes. The hydrodynamic diameter of nanocluster treated with different samples was further determined by dynamic light scattering (DLS). As shown in Figure 3a, the curve of PVA@NMIO showed a narrow peak at around 45 nm, indicating PVA@NMIO possessed good dispersity in aqueous solution. However, the curves of PVA@NMIO treated with BA/BE displayed broad peaks with different levels of right shifts, indicating that PVA@NMIO has aggregated to different degrees. These results were consistent with the aggregation observed in TEM images.

The surface structure and composition of PVA@NMIO before and after BA/BE binding were investigated by FT-IR (Figure 3b). The peaks at 1397 cm^{-1} and 1096 cm^{-1} and the broad peak at 3200−3500 cm^{-1} (blue line) were attributed to C−H bending vibration, C−O stretching vibration, and C−O−

DOI: 10.1021/acsami.5b04863
ACS Appl. Mater. Interfaces 2015, 7, 16837−16841

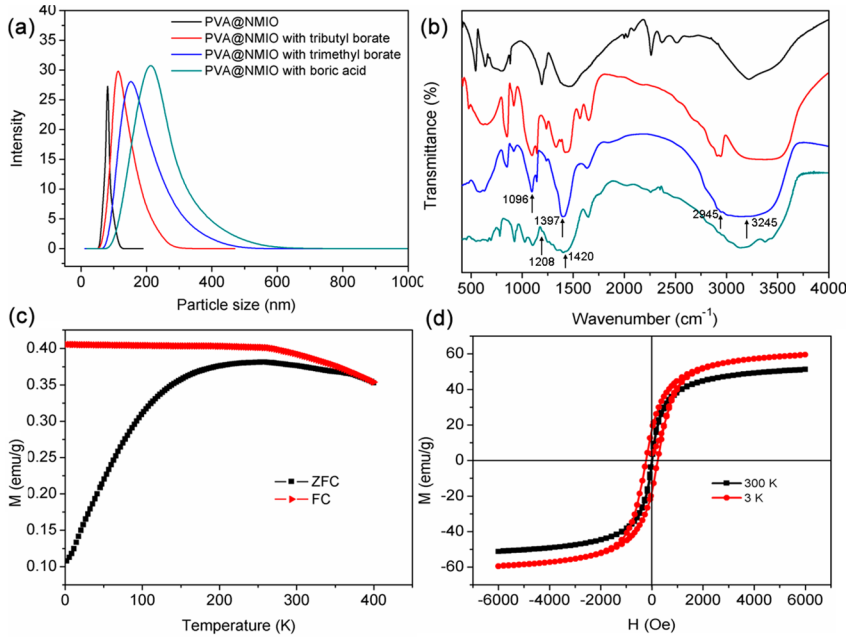

Figure 3. Particle size distribution of PVA@NMIO before and after adding BA/BE (a); the FT-IR spectra of the H3BO3 (black), PVA (red), PVA@NMIO (blue), and PVA@NMIO after adding BA (green) (b); the magnetization of PVA@NMIO measured at 3 and 300 K (c); the temperature dependence of the ZFC and FC magnetization curves for PVA@NMIO (d).

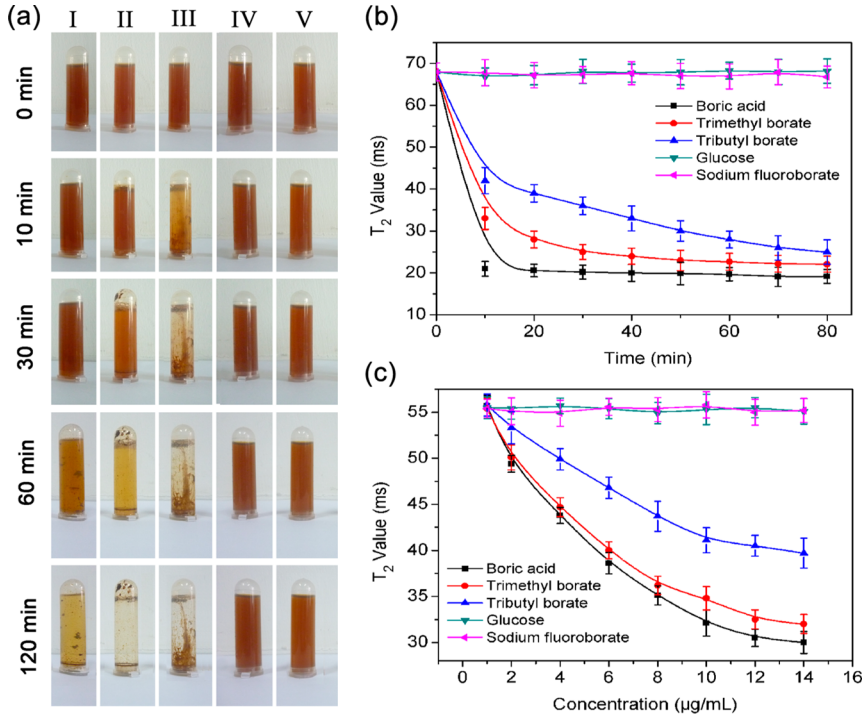

Figure 4. (a) Photos of PVA@NMIO solution (200 μg/mL) after adding 2 mg/mL of tributyl borate (I), trimethyl borate (II), boric acid (III), $NaBF_4$ (IV), and glucose (V) for different times. Sensitivity of magnetic nanosensor based on PVA@NMIO: (b) variation of the T_2 relaxation time of PVA@NMIO particles (10 μg/mL) after adding 10 μg/mL of different samples for different times; (c) dependence of the T_2 relaxation time of PVA@NMIO particles on the concentrations of different samples.

H stretching vibration, respectively. These data confirmed that the NMIO particle was successfully coated by PVA. Moreover, when BA/BE was added to PVA@NMIO dispersed solution, another two weak peaks at 1420 and 1208 cm^{-1} (green line) were observed, which were assigned to B−O stretching vibration and B−O−B bending vibration,[24,25] indicating that BA/BE was bound on the surface of PVA@NMIO.

Field-dependent magnetization curves of PVA@NMIO were recorded using a superconducting quantum interference device magnetometer with fields up to 0.6 T (Figure 3d). PVA@NMIO particles displayed superparamagnetic characteristics at 300 K, obtaining 51.8 emu/g saturation moments. In contrast, the material exhibited typically ferromagnetic hysteresis loops including coercivity and remanence at 3 K, because the

DOI: 10.1021/acsami.5b04863
ACS Appl. Mater. Interfaces 2015, 7, 16837−16841

moment randomization of PVA@NMIO particles was limited under low temperature.[26] The temperature-dependent magnetization curves of PVA@NMIO were also recorded at an applied field of 100 Oe using zero-field-cooling (ZFC) and field-cooling (FC) procedures. As shown in Figure 3c, these two curves were overlapped at high temperature but split at low temperature. The blocking temperature of PVA@NMIO particle was about 230 K with a broad peak, indicating that the nanoparticles were superparamagnetic at physiological temperature (~310 K). These results indicated PVA@NMIO possessed a good T_2-weighted MR contrast effect because the nanoparticle with good magnetic properties could cause significantly local inhomogeneities under the external magnetic field, resulting in a further reduction of the transverse relaxation time of the water proton.

To examine whether PVA@NMIO could be used as an MRS sensor to detect boron compounds with an electron-deficient boron atom, three analytes, including tributyl borate, trimethyl borate, and boric acid, were chosen. As shown in Figure 4a, the PVA@NMIO sample was a brown homogeneous suspension. However, the PVA@NMIO aggregated and precipitated over time upon the addition of BA/BE with relatively high concentration (2 mg/mL), indicating the strong interaction between BA/BE and PVA@NMIO (Figure 4aI, II, and III). It was also found that the rate of aggregation between BA and PVA@NMIO was faster than that of BE and PVA@NMIO. To investigate the selectivity of PVA@NMIO as an MRS sensor, further studies were performed by incubating the PVA@NMIO with $NaBF_4$ and glucose. $NaBF_4$ was chosen as a positive control, owing to the full electron orbits of its boron atom. Glucose acted as the negative control for its multitude of hydroxyl groups. Under this condition, the PVA@NMIO sample remained a brown homogeneous suspension (Figure 4aIV and V), confirming that there was no interaction between boron compounds and the full electron orbits of boron atom and PVA@NMIO.

The ability of PVA@NMIO to detect BA/BE was evaluated by measuring T_2 relaxation time as a function of time (Figure 4b). When PVA@NMIO particles were incubated in water, little or no change of T_2 relaxation time was observed over 3 weeks. This indicated the PVA@NMIO particles were highly stable, which ensured the magnetic particles possess a sensitive spin−spin relaxation time (T_2) for monitoring small signal change by T_2 measurement. T_2 relaxation time decreased when BA was added to a PVA@NMIO sample, and there was ~45 ms change in T_2 relaxation time within 20 min (Figure 4b). The reduction in T_2 relaxation time was also observed when BE including trimethyl borate and tributyl borate was added to a PVA@NMIO sample. However, the T_2 reduction rate and magnitude change for BA-PVA@NMIO were faster/larger than those of BE-PVA@NMIO, which was consistent with the aggregation observed in Figure 4a. We further explored the selectivity of PVA@NMIO by measuring T_2 upon the addition of glucose and $NaBF_4$. As expected, the incubation $NaBF_4$ with PVA@NMIO did not alter the T_2 relaxation time, suggesting that $NaBF_4$ with full boron coordination did not react with the hydroxyl groups of PVA@NMIO. As shown in Figure 4c, T_2 relaxation time reduced as BE/BA concentration increased. Control samples including $NaBF_4$ and glucose incubated with PVA@NMIO showed no T_2 change, as expected.

The feasibility of conducting high-throughput screening for BA/BE was also investigated using magnetic resonance (MR) imaging. MR images (T_2 maps) were obtained for 48 MRS samples simultaneously in a 96-well plate (Figure 5). It could be seen that MR images significantly darkened with increasing concentrations and time after adding BA. In contrast, MR images of control samples showed no variation. Data analysis was completed in approximately 5 min, indicating that several thousands of samples could be measured per day by MR detector. In addition, the MRS system might also provide a potential application of detecting trace boron in an organism using imaging, because MR imaging could noninvasively obtain 3D tomographic images with exquisite tissue contrast. Related experiments are currently in process.

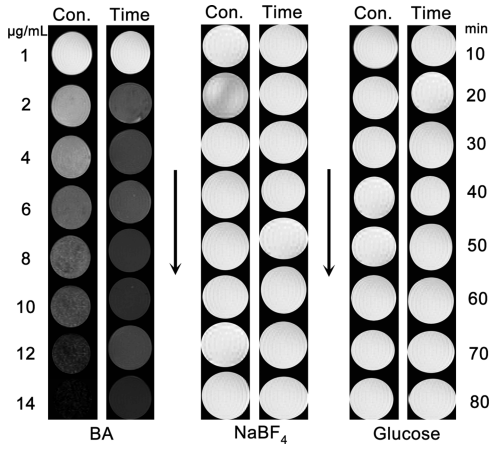

Figure 5. Magnetic resonance T_2 maps of MRS samples after adding different concentrations of samples for 30 min and adding samples (10 μg/mL) for different times.

CONCLUSIONS

In summary, a MRS system based on in situ synthesized superparamagnetic PVA@NMIO particles has been developed and used as a new tool for the detection of BA/BE. The addition of BA/BE induced the aggregation of PVA@NMIO particles and reduced the T_2 relaxation time of the water. This MRS system showed a good sensitivity and selectivity for the high-throughput detection of BA/BE. It is envisioned that this MRS sensor may facilitate research on food safety or biological effects related to boron.

AUTHOR INFORMATION

Corresponding Authors

*E-mail: dqcai@ipp.ac.cn (D.C.).
*E-mail: zcheng@seas.upenn.edu (Z.C.).
*E-mail: zywu@ipp.ac.cn (Z.W.).

Author Contributions

⊥G.Z. and S.L. are cofirst authors.

Notes

The authors declare no competing financial interest.

ACKNOWLEDGMENTS

The authors acknowledge financial support from the National Key Foundation for Exploring Scientific Instrument of China (No. 2013YQ17058507), the National Natural Science Foundation of China (No. 21407151, No. 81201068), the Key Program of Chinese Academy of Sciences (No. KSZD-EW-Z-022-05), and the Science and Technology Service

DOI: 10.1021/acsami.5b04863
ACS Appl. Mater. Interfaces 2015, 7, 16837−16841

Project of Chinese Academy of Sciences (No. KFJ-EW-STS-067).

REFERENCES

(1) Barranco, W. T.; Eckhert, C. D. Boric Acid Inhibits Human Prostate Cancer Cell Proliferation. *Cancer Lett.* **2004**, *216*, 21−29.
(2) Argust, P. Distribution of Boron in the Environment. *Biol. Trace Elem. Res.* **1998**, *66*, 131−143.
(3) Hristoforou, E.; Vlachos, D. S. *Key Engineering Materials*; Trans Tech. Publications: Zurich, 2012; Vol. *605*, pp 356−359.
(4) Kumar, G.; Srivastava, N. Genotoxic Effects of Two Commonly Used Food Additives of Boric Acid and Sunset Yellow in Root Meristems of Trigonella Foenum-Graecum. *Iran. J. Environ. Health Sci. Eng.* **2011**, *8*, 361−366.
(5) Sah, R. N.; Brown, P. H. Boron Determination-A Review of Analytical Methods. *Microchem. J.* **1997**, *56*, 285−304.
(6) Kataoka, H.; Okamoto, Y.; Tsukahara, S.; Fujiwara, T.; Ito, K. Separate Vaporization of Boric Acid and Inorganic Boron from Tungsten Sample Cuvette-Tungsten Boat Furnace Followed by the Detection of Boron Species by Inductively Coupled Plasma Mass Spectrometry and Atomic Emission Spectrometry (ICP-MS and ICP-AES). *Anal. Chim. Acta* **2008**, *610*, 179−185.
(7) Taler, G.; Eliav, U.; Navon, G. Detection and Characterization of Boric Acid and Borate Ion Binding to Cytochrome C using Multiple Quantum Filtered NMR. *J. Magn. Reson.* **1999**, *141*, 228−238.
(8) Fang, Z. Nonequilibrated Sample Manipulation-The Essence of Flow-Injection Analysis. *Microchem. J.* **1992**, *45*, 137−142.
(9) Hill, C. J.; Lash, R. P. Ion Chromatographic Determination of Boron as Tetrafluoroborate. *Anal. Chem.* **1980**, *52*, 24−27.
(10) Zhang, G. L.; Gao, J. L.; Qian, J. C.; Cai, D. Q.; Zheng, K.; Yu, Z. W.; Wang, J. F.; Zhong, K.; Zhang, X.; Wu, Z. Y. A Multifunctional Magnetic Composite Material as a Drug Delivery System and a Magnetic Resonance Contrast Agent. *Part. Part. Syst. Charact.* **2014**, *31*, 976−984.
(11) Ma, Q.; Nakane, Y.; Mori, Y.; Hasegawa, M.; Yoshioka, Y.; Watanabe, T. M.; Gonda, K.; Ohuchi, N.; Jin, T. Multilayered, Core/Shell Nanoprobes Based on Magnetic Ferric Oxide Particles and Quantum Dots for Multimodality Imaging of Breast Cancer Tumors. *Biomaterials* **2012**, *33*, 8486−8494.
(12) Thorek, D. L.J.; Tsourkas, A. Size, Charge and Concentration Dependent Uptake of Iron Oxide Particles by Non-Phagocytic Cells. *Biomaterials* **2008**, *29*, 3583−3590.
(13) Perez, J. M.; Josephson, L.; O'Loughlin, T.; HÖgemann, D.; Weissleder, R. Magnetic Relaxation Switches Capable of Sensing Molecular. *Nat. Biotechnol.* **2002**, *20*, 816−820.
(14) Tsourkas, A.; Hofstetter, O.; Hofstetter, H.; Weissleder, R.; Josephson, L. Magnetic Relaxation Switch Immunosensors Detect Enantiomeric Impurities. *Angew. Chem., Int. Ed.* **2004**, *43*, 2395−2399.
(15) Kim, G. Y.; Josephson, L.; Langer, R.; Cima, M. J. Magnetic Relaxation Switch Detection of Human Chorionic Gonadotrophin. *Bioconjugate Chem.* **2007**, *18*, 2024−2028.
(16) Nasongkla, N.; Bey, E.; Ren, J.; Ai, H.; Khemtong, C.; Guthi, J. S.; Chin, S. F.; Sherry, A. D.; Boothman, D. A.; Gao, J. M. Multifunctional Polymeric Micelles as Cancer-Targeted, MRI-Ultrasensitive Drug Delivery Systems. *Nano Lett.* **2006**, *6*, 2427−2430.
(17) Frey, N. A.; Peng, S.; Cheng, K.; Sun, S. H. Magnetic Nanoparticles: Synthesis, Functionalization, and Applications in Bioimaging and Magnetic Energy Storage. *Chem. Soc. Rev.* **2009**, *38*, 2532−2542.
(18) Li, J. C.; Shi, X. Y.; Shen, M. W. Hydrothermal Synthesis and Functionalization of Iron Oxide Nanoparticles for MR Imaging Applications. *Part. Part. Syst. Charact.* **2014**, *31*, 1223−1237.
(19) Qiao, R.; Yang, C.; Gao, M. Superparamagnetic Iron Oxide Nanoparticles: From Preparations to in Vivo MRI Applications. *J. Mater. Chem.* **2009**, *19*, 6274−6293.
(20) Yuan, Y.; Rende, D.; Altan, C. L.; Bucak, S.; Ozisik, R.; Borca-Tasciuc, D. A. Effect of Surface Modification on Magnetization of Iron Oxide Nanoparticle Colloids. *Langmuir* **2012**, *28*, 13051−13059.
(21) Zhao, M.; Josephson, L.; Tan, Y.; Weissleder, R. Magnetic Sensors for Protease Assays. *Angew. Chem., Int. Ed.* **2003**, *42*, 1375−1378.
(22) Perez, J. M.; O'Loughlin, T.; Simeone, F. J.; Weissleder, R.; Josephson, L. DNA-Based Magnetic Nanoparticle Assembly Acts as a Magnetic Relaxation Nanoswitch Allowing Screening of DNA-Cleaving Agents. *J. Am. Chem. Soc.* **2002**, *124*, 2856−2857.
(23) Cheng, Z. L.; Tsourkas, A. Monitoring Phospholipase A2 Activity with Gd-encapsulated Phospholipid Liposomes. *Sci. Rep.* **2014**, *4*, 6958.
(24) Shen, P.; Xia, Y. Synthesis-Modification Integration: One-Step Fabrication of Boronic Acid Functionalized Carbon Dots for Fluorescent Blood Sugar Sensing. *Anal. Chem.* **2014**, *86*, 5323−5329.
(25) Brewer, S. H.; Allen, A. M.; Lappi, S. E.; Chasse, T. L.; Briggman, K. A.; Gorman, C. B.; Franzen, S. Infrared Detection of a Phenylboronic Acid Terminated Alkane Thiol Monolayer on Gold Surfaces. *Langmuir* **2004**, *20*, 5512−5520.
(26) Zhang, F.; Braun, G. B.; Pallaoro, A.; Zhang, Y. C.; Shi, Y. F.; Cui, D. X.; Moskovits, M.; Zhao, D. Y.; Stucky, G. D. Mesoporous Multifunctional Upconversion Luminescent and Magnetic "Nanorattle" Materials for Targeted Chemotherapy. *Nano Lett.* **2012**, *12*, 61−67.

DOI: 10.1021/acsami.5b04863
ACS Appl. Mater. Interfaces 2015, 7, 16837−16841